



Science Arts & Métiers (SAM)

is an open access repository that collects the work of Arts et Métiers Institute of Technology researchers and makes it freely available over the web where possible.

This is an author-deposited version published in: <https://sam.ensam.eu>
Handle ID: <http://hdl.handle.net/10985/19787>

To cite this version :

Joffrey VIGUIER, Bertrand MARCON, Jean-Claude BUTAUD, Louis DENAUD, Robert COLLET -
Panel Shear of Plywood in Structural Sizes - Assessment Improvement Using Digital Image
Correlation - Experimental Techniques p.0 - 2021

Any correspondence concerning this service should be sent to the repository

Administrator : archiveouverte@ensam.eu





Panel Shear of Plywood in Structural Sizes - Assessment Improvement Using Digital Image Correlation

J. Viguier¹ · B. Marcon¹ · J. C. Butaud¹ · L. Denaud¹ · R. Collet¹

Received: 25 June 2019 / Accepted: 8 December 2020
 © Springer Nature Switzerland AG part of Springer Nature 2020

Abstract

This paper introduces a new test configuration for the determination of panel shear properties in structural sizes. This original test configuration has been successfully applied to calculate the shear properties of beech plywood. A numerical model has been developed to evaluate the influence of such a novel setup in comparison to the common standard. The research includes the mechanical characterization of a total of 36 samples using Digital Image Correlation (DIC) to measure the in plane displacements. The use of DIC has been proven to be efficient to measure the shear properties and also acts as a tool to ensure that the sollicitation was adequate during the test. Finally, the results highlight the interest to actually perform the proposed test instead of using the alternative density-based equivalencies provided by the standards.

Keywords Shear · DIC · Beech · Plywood

Introduction

Plywood is often used in the construction sector. In particular, high quality beech plywood could exhibit great features to be used in the construction for plywood gussets in nailed or glued trusses or as a web of I-Joist. Therefore obtaining reliable shear properties for plywood is essential to ensure security and cost efficiency in the legal range of the building standards. The measured shear properties has not been found to be a constant value [1], but appears to be affected by the method of shear properties determination even when controlling all factors which normally affect the mechanical properties of wood. The evaluation of shear properties has conducted to create a wide range of standardized and non-standardized test methods (two rails, plate shear, bending tests, torsion, ...). Among those, the two rails type seems to be preferred in order to test plywood in structural size. During this test, the load is transferred to the specimen through two pair of rails glued or bolted parallel to its longer edge in such a way that the shear is nearly pure in the central area. Several studies [2–6] have

been conducted over the years to develop or assessing the difference between two-rails type tests.

The area exposed to shear has been kept nearly constant over the years to a rectangle of approximately 200 by 600 mm². Different strategies to perform this test have been experienced, all of them requiring complicated apparatus (see Fig. 1). In the latest European standard (EN 789 [7]), this area has been changed to a more complicated shape with a slightly lower area (see Fig. 1(c)) but the principle and the complexity remain constant. This complexity probably causes the lack of values issued from plywood performance declaration of the majority of the plywood panel manufacturers. Indeed, the producers prefer to use density equivalencies given in EN 12369-2 [8] to provide shear properties even if they are very penalizing and do not reflect the true mechanical properties of plywood panels especially in the case of beech.

Panels shear modulus is usually measured using a Linear Variable Differential Transformer (LVDT) orientated by 45° across the central area (symbolized by a rectangle in Fig. 1) on each side of the specimen and then averaged. Timbers shear modulus can also be determined through flexural [9] or torsional [10] vibration mechanical tests with accelerometers and more or less complex finite elements analysis (FEA). In this study, Digital Image Correlation (DIC) is proposed as an alternative to the fixation of LVDT and as a substantial improvement to measure those displacements. In the past 30 years, DIC has proved to be

✉ J. Viguier
 joffrey.viguier@gmail.com

¹ LaBoMaP, Arts et Metiers Institute of Technology, LaBoMaP, HESAM Université, rue Porte de Paris, F-71250, Cluny, France



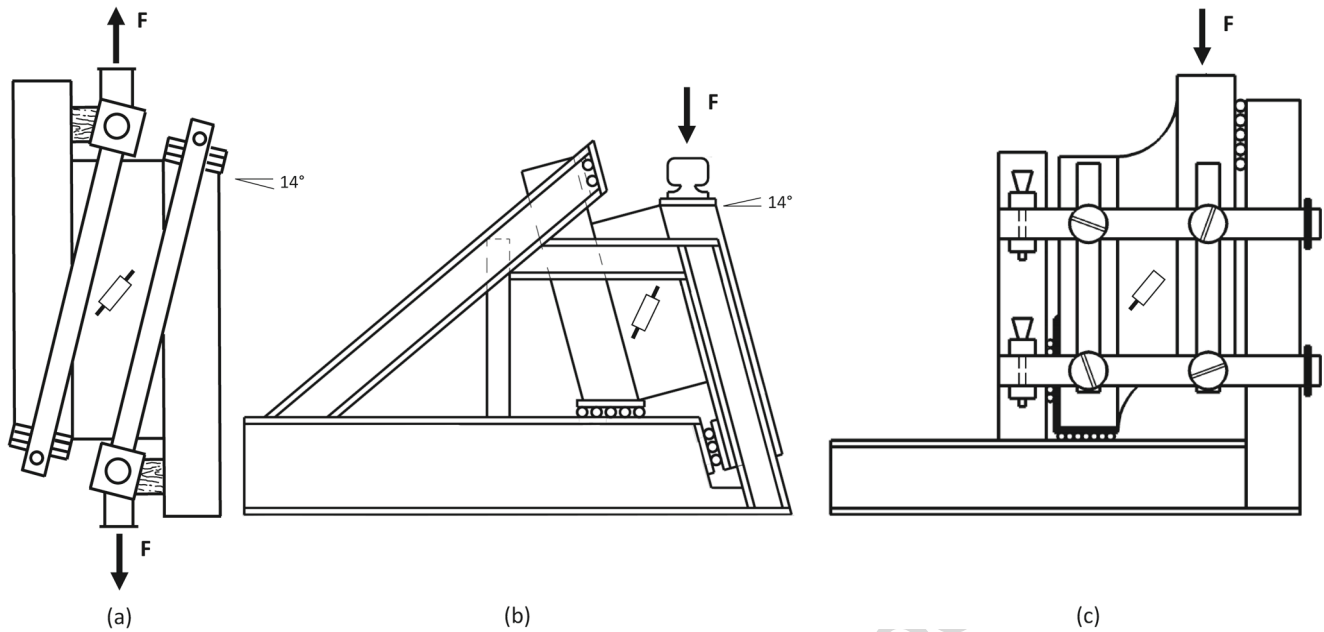


Fig. 1 Different two-rails configuration tests used or in use within the past 30 years

48 a very valuable non-invasive tool for full-field displacement
 49 measurements [11–14] and its accuracy has been proven
 50 [15]. The use of DIC in the field of wood testing is
 51 increasing [16–18].

52 The main objective of the present study is to propose a
 53 simpler method to determine the shear properties of wooden
 54 panels and more particularly plywood ones. In addition an
 55 experimental part designed to validate the modified test
 56 using full field measurements, finite elements numerical
 57 simulations have been used to determine the influence of
 58 using the proposed test method on the mechanical properties
 59 of the plywood panels.

60 **Materials and Methods**

61 **Sampling**

62 A total of 18 beech plywood panels were used for this
 63 study and two different thicknesses (18 and 25 mm with
 64 respectively 9 and 11 plies) have been studied. Samples
 65 were cut using a three-axis router machine according to
 66 the shape described in Fig. 2. In order to define a test
 67 which can be performed easier than the one described in
 68 the standard [7], involving a less bulky setup, the chosen
 69 strategy was to tilt the sample. For the experimental part,
 70 the angle α has been taken equal to 18° in such a way
 71 that the moment is nearly equal to 0. In doing so, the
 72 special apparatus described in the standard was not needed
 73 anymore and the initially complex test looks like a simple
 74 self balanced compression test. Four Douglas-fir timber

rails with a thickness equals to 35 mm have then been glued
 using polyvinyl acetate (PVAC) to each specimen to avoid
 buckling of the sample during the test as required by the
 standard [7]. Two samples have been cut from each panel
 : one having its external ply with fiber along the longest
 dimension and the second one perpendicular to its longest
 dimension. Finally, 36 samples have been made.

82 **Mechanical Test and Displacements Measurement**

83 The tests were performed with a Zwick Roell static material
 84 testing machine with a 250 kN load cell. The load was
 85 applied on the top surface of the timber rails with an
 86 adjusted application rate, so that the maximum load was
 87 reached within 300 ± 120 s according to EN 789 [7].
 88 In practice, the loading rate has been chosen equals to 2
 89 mm/min. The shear deformation was measured on both
 90 faces in the middle of the specimen using 2D digital image
 91 correlation. Images of both faces and their corresponding
 92 load were recorded during the whole test. Digital frames
 93 of both sides of the specimen were recorded using two
 94 Basler ace acA1920-155um type imagers equipped with
 95 Pentax Ricoh FL-CC3516-2M - 1.6 / 35 mm lenses. Those
 96 cameras exhibit a resolution of 1920 by 1200 square pixels
 97 with a pitch size of $5.86e^{-3}$ mm². The observed area was
 98 set to 211 by 132 mm² thanks to extension tubes with a
 99 working distance (standoff distance) of 1 meter. The scene
 100 was illuminated using identical white LED projectors on
 101 both sides and a built-in lens diaphragm used to reach
 102 identical grey level repartition histograms for both sides of
 103 the specimen. The geometrical centres had been marked

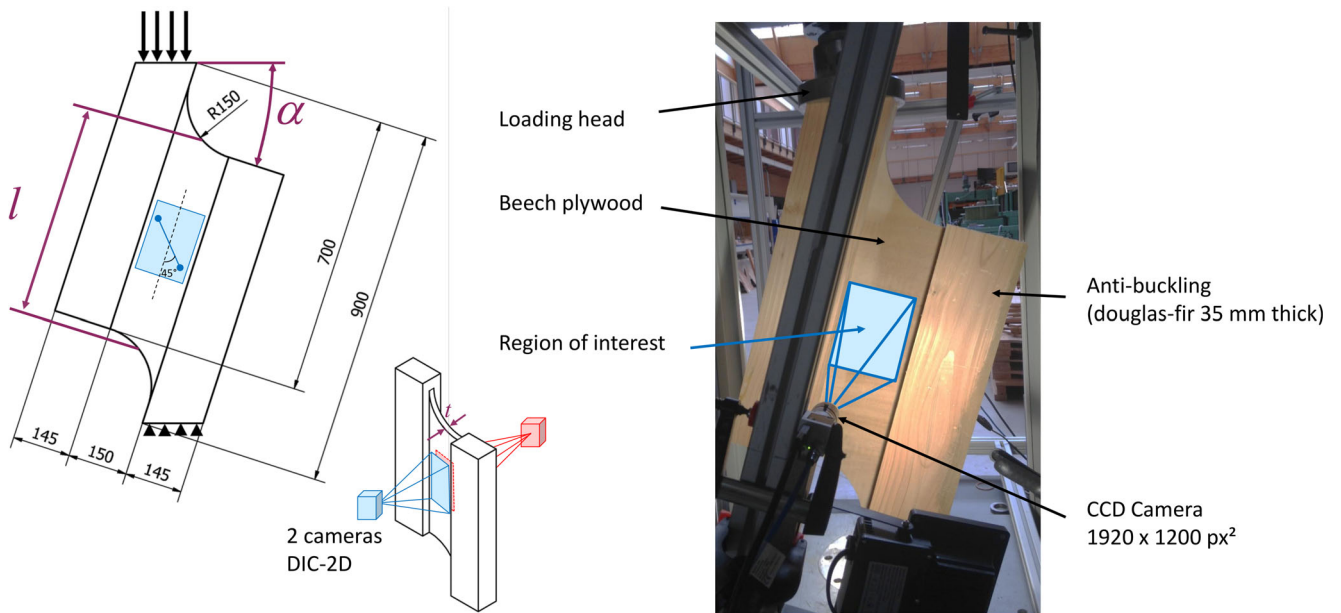


Fig. 2 Experimental test setup

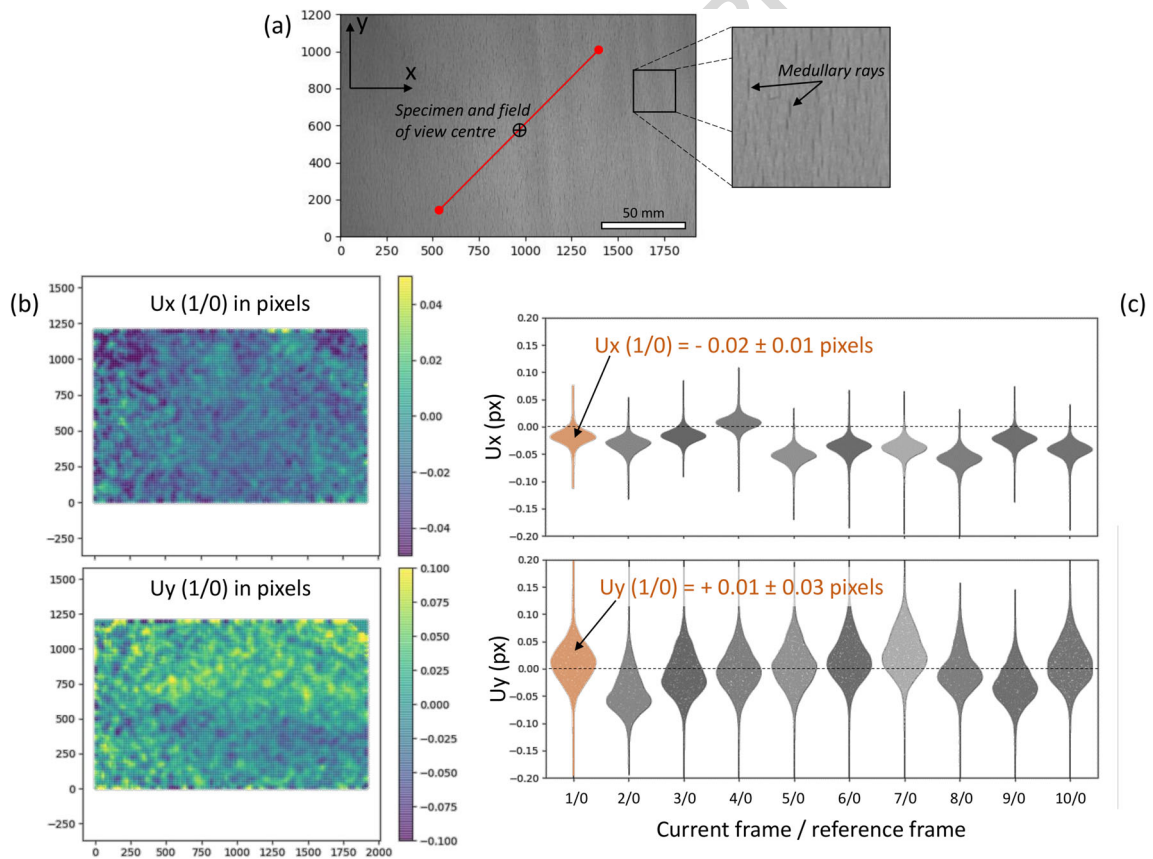


Fig. 3 **a** beech natural pattern for DIC on one sample showing medullary rays (elliptical darker shapes), **b** corresponding X-and Y-displacement fields obtained between the first image and the reference image, **c** DIC pseudostatic accuracy assessment from 10 consecutive images taken free from loading

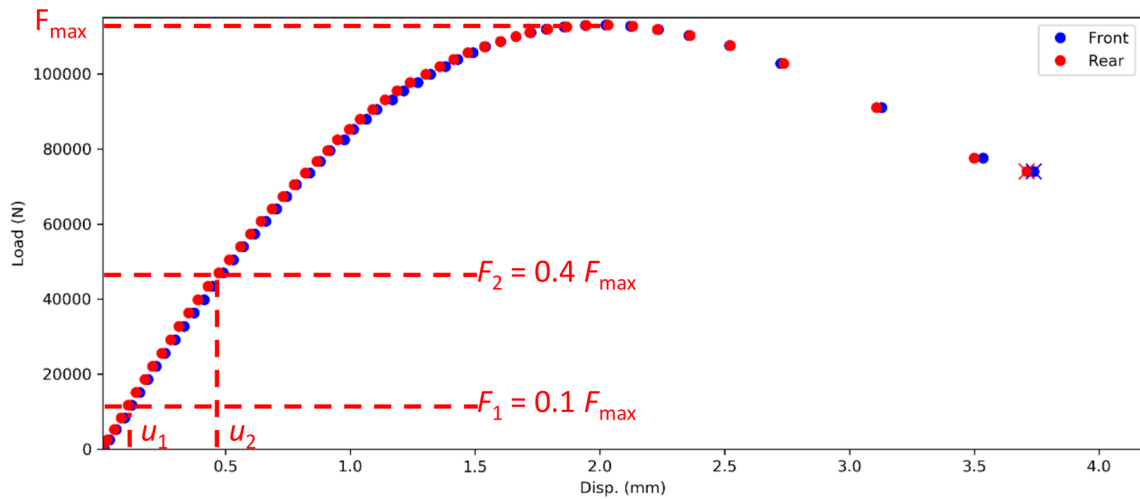


Fig. 4 Typical load-displacement curves (front and rear) used for the panel shear properties assessments. The displacement represents the distance measured by DIC between two points located on the compression diagonal at 45° to the rails passing through the centre of the shear area

precisely on both sides of the specimen and centred on both camera respective fields of view before tests were performed (see Fig. 3(a)). Moreover, the alignment of the camera axis with the specimen ones, as represented in the Fig. 2, was ensured by imposing their correspondence with the anti-buckling beams, and the camera orientation (sensor parallel with the observed area) was checked using a grid calibration plate. The magnification factor obtained with such experimental set up was 9.08 px/mm (or 0.11 mm/px). Hardware and software resources have been developed specifically to record simultaneously the load value and its corresponding pictures. The experimental test setup is described in Fig. 2.

The principle of Digital Image Correlation is to compare digitized images of non-deformed specimen (reference) to multiple images of the same specimen while applying the loading to obtain the full-field displacement. An important element of the measurement procedure is the image analysis software package which is supposed to provide an apparent 2-D displacement field that maps a so-called "reference image" to a "deformed image" at a discrete set of positions, according to the principle of optical flow conservation. The displacement was computed using the image analysis software, DaVIS 10.0.5, by LaVision. In the case of this

study, no surface preparation of the observed area has been done, the medullary rays of beech as shown in (Fig. 3(b)) have been directly used as the pattern from which to correlate the images between two successive loading steps. The subsize and the stepsize have been taken equal to 51 and 17 pixels respectively. The region of interest is shown in Fig. 2. The image acquisition frequency was fixed at 0.2 Hz.

The natural pattern the beech plywood featured, see (Fig. 3(a)), appeared as really satisfying among the different surface preparation considering the difficulty to master the paint application on big amount of samples compared to the accuracy required for the shear modulus determination (some details regarding this will be discussed in Section "Mechanical Properties Calculation"). Nonetheless, the natural pattern of beech veneer is anisotropic due to the presence of elliptic and oriented medullary rays affecting the correlation error which becomes anisotropic correspondingly.

Table 1 Material properties used in finite elements analysis

Property	Ply material (beech) [20]	Wood support (Douglas fir) [21]
E_X (MPa)	14000	14740
E_Y (MPa)	1160	737
ν_{XY}	0.45	0.45
G_{XY} (MPa)	1080	1150

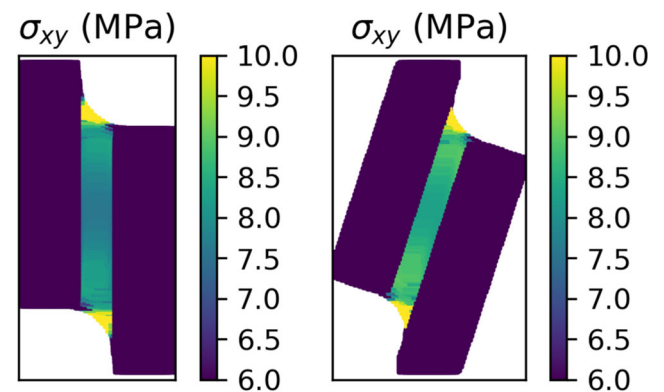


Fig. 5 Comparison of the modeled strain field obtained from vertical and tilted samples

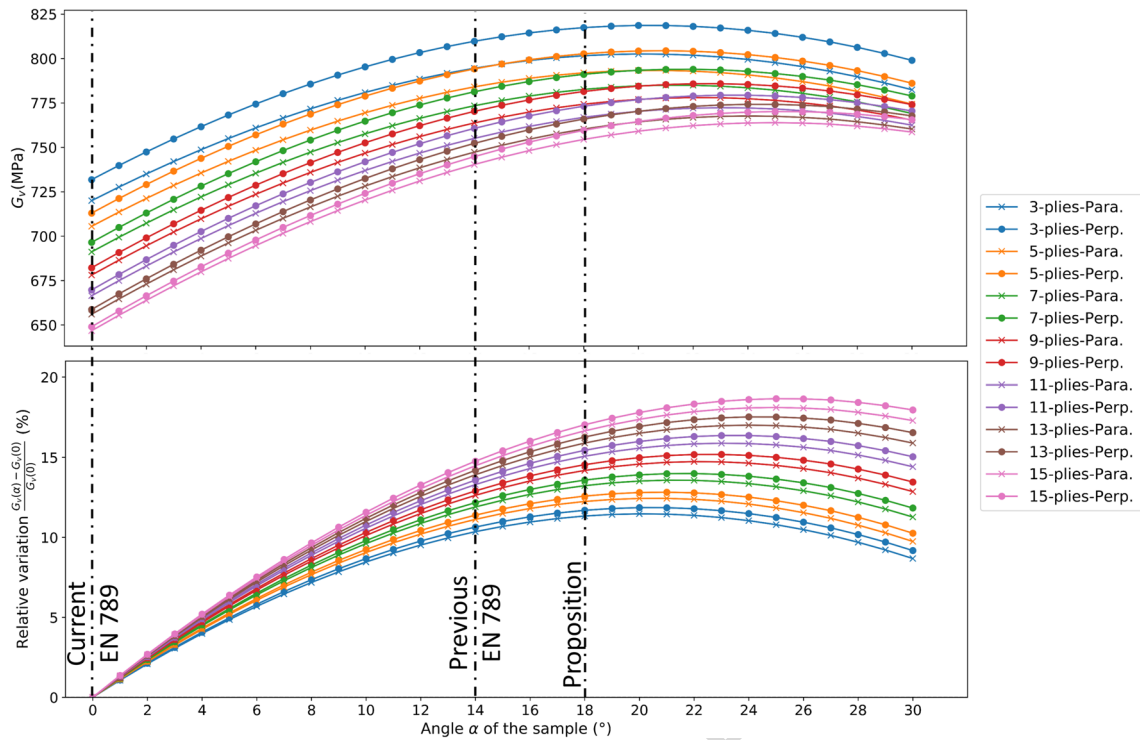


Fig. 6 Influence of tilting the sample at different angle on the calculation of G_v . The results for two types of sample (Parallel and Perpendicular) and different thicknesses are presented. The upper part shows the calculated G_v and the lower part the relative variation observed with the configuration without tilting the sample

146 The average correlation error is determined using the
 147 10 images taken before the loading is applied for each
 148 sample, performing a DIC computation on them under the
 149 exact same calculation settings (subset size 51 pixels and
 150 step size 17 pixels), and extracting the standard deviation
 151 at 68% confidence interval of the X- and Y-displacement
 152 fields obtained for those non-deformed configurations. An
 153 example is provided in (Fig. 3(b)). Thus, the average
 154 displacement field error, arising from the whole samples
 155 batch on both sides, were $\pm 4.4E^{-3}$ mm (± 0.02 pixel)
 156 and $\pm 2.2E^{-3}$ mm (± 0.01 pixel) respectively for the
 157 medullary rays direction and its normal one displayed by
 158 (Fig. 3(b) and (c)). Those values embed the pattern quality,
 159 the enlightenment intensity variations and the eventual
 160 whole system vibrations (rigid body displacement between
 161 the sample and the cameras). The influence of this error on
 162 the calculation of the shear modulus will be discussed later.

163 Mechanical Properties Calculation

164 The calculation of the shear modulus is based on
 165 load-displacement curves. The displacement is measured
 166 between two selected positions on the images. Those two
 167 positions were located on the compression diagonal at 45°
 168 to the rails passing through the centre of the shear area. The
 169 distance between the two points is equal to 120 mm and

170 corresponds to the theoretical position of the extensometer
 171 prescribed in EN 789 [7] (see Fig. 2).

172 The invasive attachment of a physical extensometer with
 173 pins inserted in holes is not necessary thanks to the use of
 174 DIC. An example on a load-displacement curves obtained
 175 on the two faces of the sample is described in Fig. 4. The
 176 section of the graph between $0.1F_{max}$ and $0.4F_{max}$ is
 177 used for a linear regression analyses and the panel shear
 178 modulus of rigidity is then calculated using (equation (1)).
 179 This equation is similar to the one given in the standard
 180 except for the $\cos(\alpha)$ term introduced to take into account
 181 the tilting angle [7].

$$G_v = \frac{0.5\cos(\alpha)(F_2 - F_1)l_1}{(u_2 - u_1)lt} \quad (1)$$

182 where:

- 183 – $(F_2 - F_1)$ is the increment of load between $0.1F_{max}$ and
 184 $0.4F_{max}$ in N,
- 185 – $(u_2 - u_1)$ is the increment of deflection corresponding
 186 to $(F_2 - F_1)$ using a linear regression in mm,
- 187 – l_1 is the distance between the two selected points and is
 188 equal to 120 mm,
- 189 – l is the length of the test piece measured along the centre
 190 line of the shear area (including the radius section) in
 191 mm,

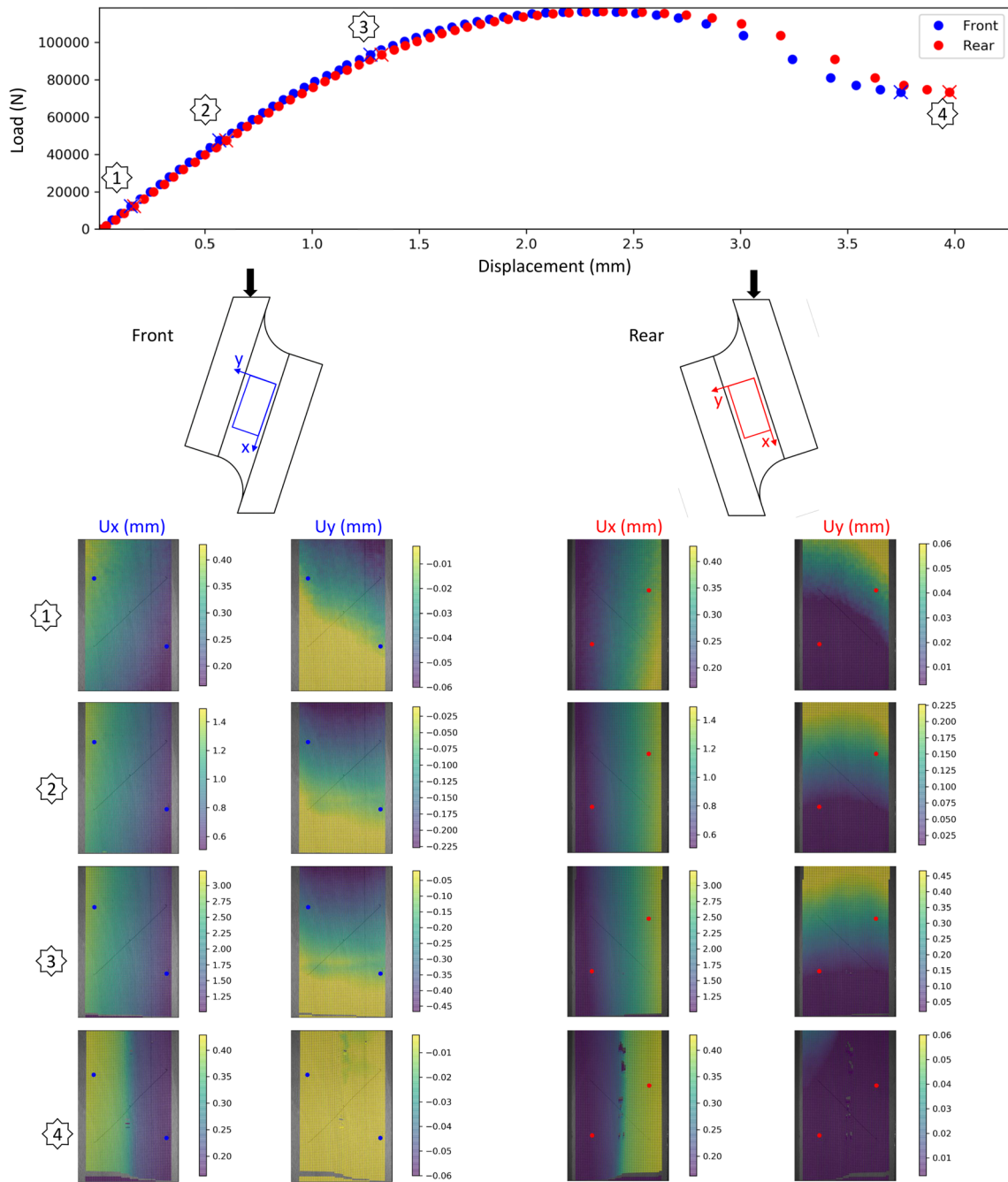


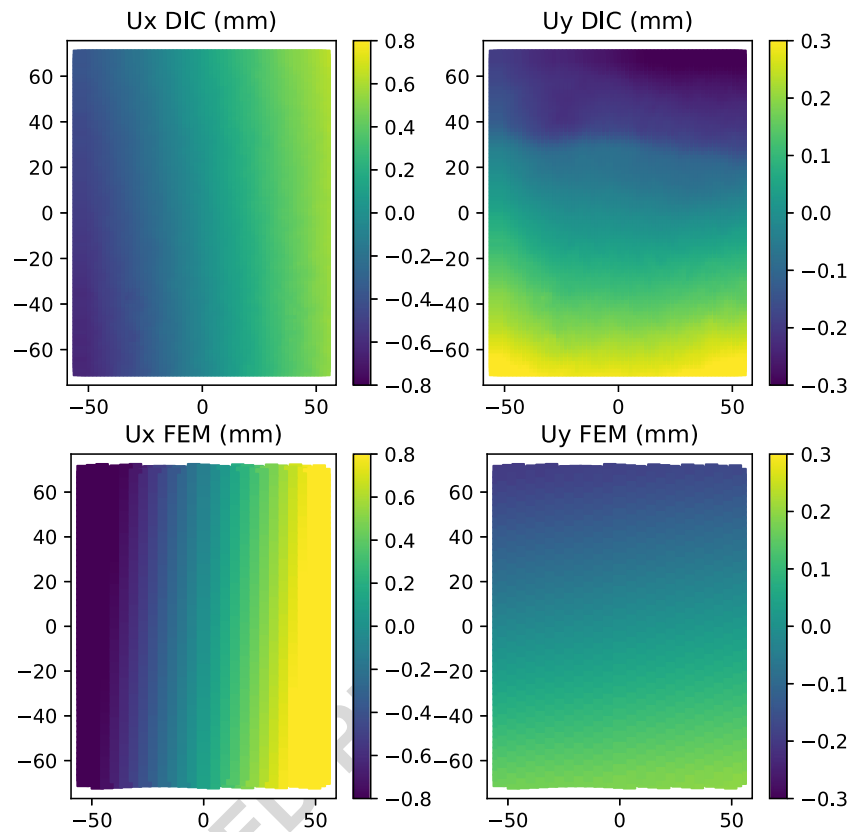
Fig. 7 Typical results of a shear test. The upper part represents the load-displacement curve during the test. Four levels of solicitation are highlighted and their respective displacement fields for both sample sides and two directions are presented in the lower part

192 – t is the average thickness of the test piece measured at
 193 two points along the centre line of the shear area in mm,
 194 – α is the tilting angle of the sample in $^{\circ}$.

195 An analysis of the error sources to determine the shear
 196 modulus G_v from (equation (1)) leads to a relative error on

the shear modulus of 1.4 % with the following individual 197
 error (experimentally determined or from device calibration 198
 certificates): $\Delta\alpha = \pm 1^{\circ}$; $\Delta F = \pm 0.5\% F = \pm 344$ N; 199
 $\Delta u = \pm 4.9E-3$ mm; $\Delta l_1 = \pm 0.5$ mm; $\Delta l = \pm 1$ mm; Δt 200
 $= \pm 0.01$ mm. This determined G_v error is mostly affected 201
 by the displacement one but remains very low, sustaining 202

Fig. 8 Comparison of displacements fields obtained on the front side experimentally by DIC and numerically by FEM



203 the applicability of DIC method using directly the natural
 204 beech wood aspect (medullary rays) as pattern (no surface
 205 preparation as paint speckle needed).

206 The panel shear strength is calculated from (equation (2))
 207 where F_{max} is the maximum load applied up to failure. In this
 208 case too the equation only differs by the $\cos(\alpha)$ term [7].

$$f_v = \frac{F_{max} \cos(\alpha)}{lt} \quad (2)$$

209 **Numerical Model**

210 To evaluate the influence of the test modification, a
 211 model has been developed using quadratic triangular
 212 elements (6-nodes) with orthotropic material properties.
 213 The finite element solver used for this study is CAST3M
 214 2019 [19], the mechanical software developed by the
 215 CEA (French Atomic Energy and Alternative Energies
 216 Commission). The grain directions between the different
 217 plies were alternatively 0° and 90° to fit with plywood
 218 panel composition. The performed simulations were linear
 219 regarding the material properties and deflections. The
 220 boundary conditions were as follows: for the lower support,
 221 displacements were locked in both directions (X and Y),
 222 and in the upper support displacements were locked in
 223 horizontal direction (X). The tilting angle of the sample
 224 varies between 0° and 30° , and the number of plies
 225 varies between 3 and 15. The thickness of each ply has been

226 taken equal to 2 mm. The material properties used in the
 227 calculations are shown in Table 1 and were taken from the
 228 literature [20, 21]. X and Y directions being respectively the
 229 fiber direction and the direction perpendicular to the fiber.
 230 Given the purpose of the model, the interface between the
 231 plies is not modeled.

232 In addition, two types of specimens were modeled in
 233 a similar way to the normative recommendations: test
 234 specimens with their face grain angle oriented parallel to
 235 the load (called type Parallel), and specimens with their face
 236 grain angle oriented perpendicular to the load (called type
 237 Perpendicular).

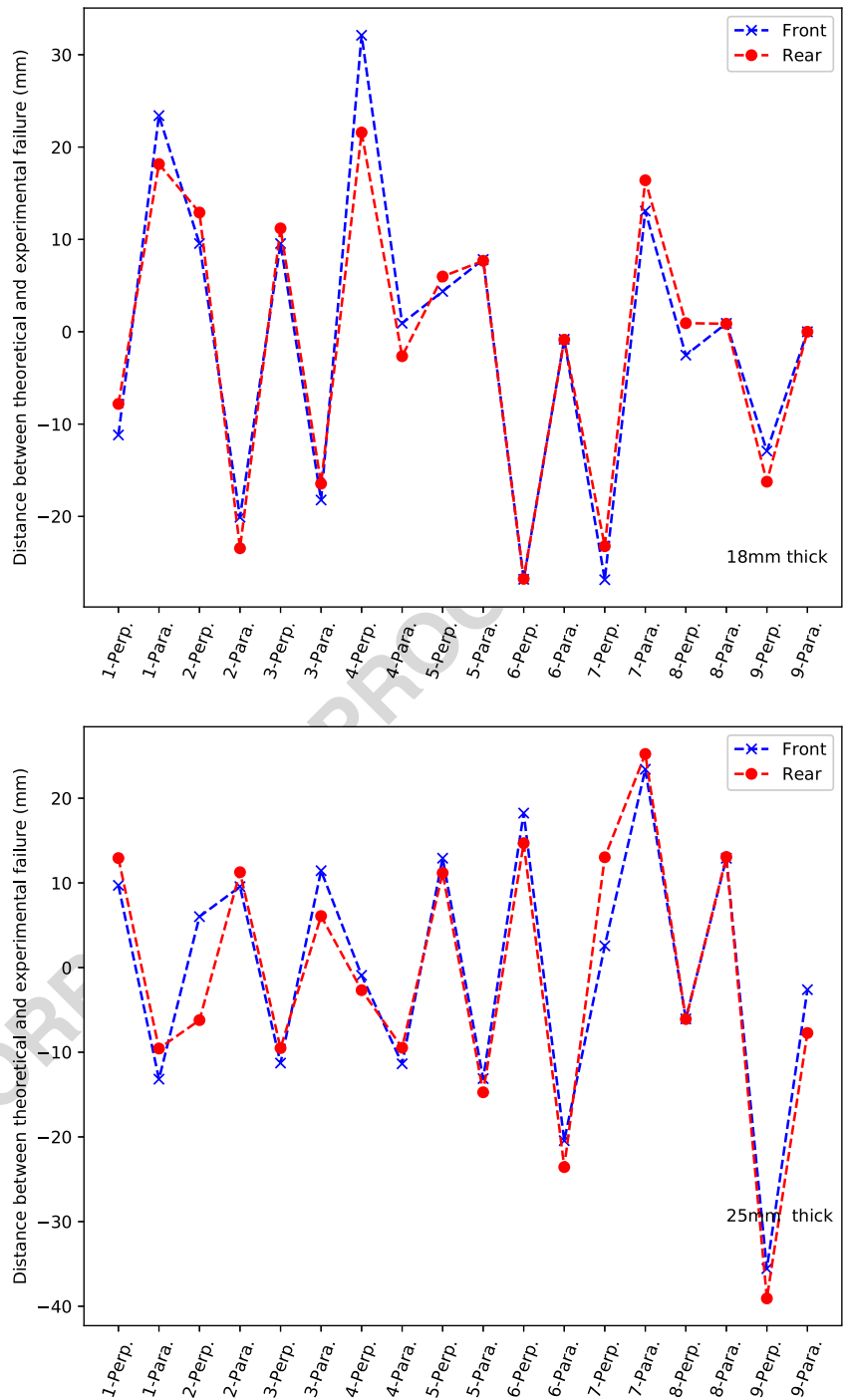
238 **Results and Discussions**

239 **Results of the Numerical Model**

240 The comparison of the shear stress fields, for the same
 241 displacement of the loading head, obtained thanks to the
 242 FEM after tilting the sample is given in Fig. 5. The different
 243 fields were really close to each other either quantitatively
 244 or qualitatively. The shear stress in the middle part of the
 245 sample is nearly constant in both cases and validate the
 246 sample tilting strategy.

247 The shear modulus of rigidity calculated for each
 248 simulation is presented in Fig. 6. As one of the model

Fig. 9 Distance between the failure position identified using DIC and the geometric centre of the sample. The upper part is related to 18 mm thick samples and the lower part show the results for 25 mm thick samples



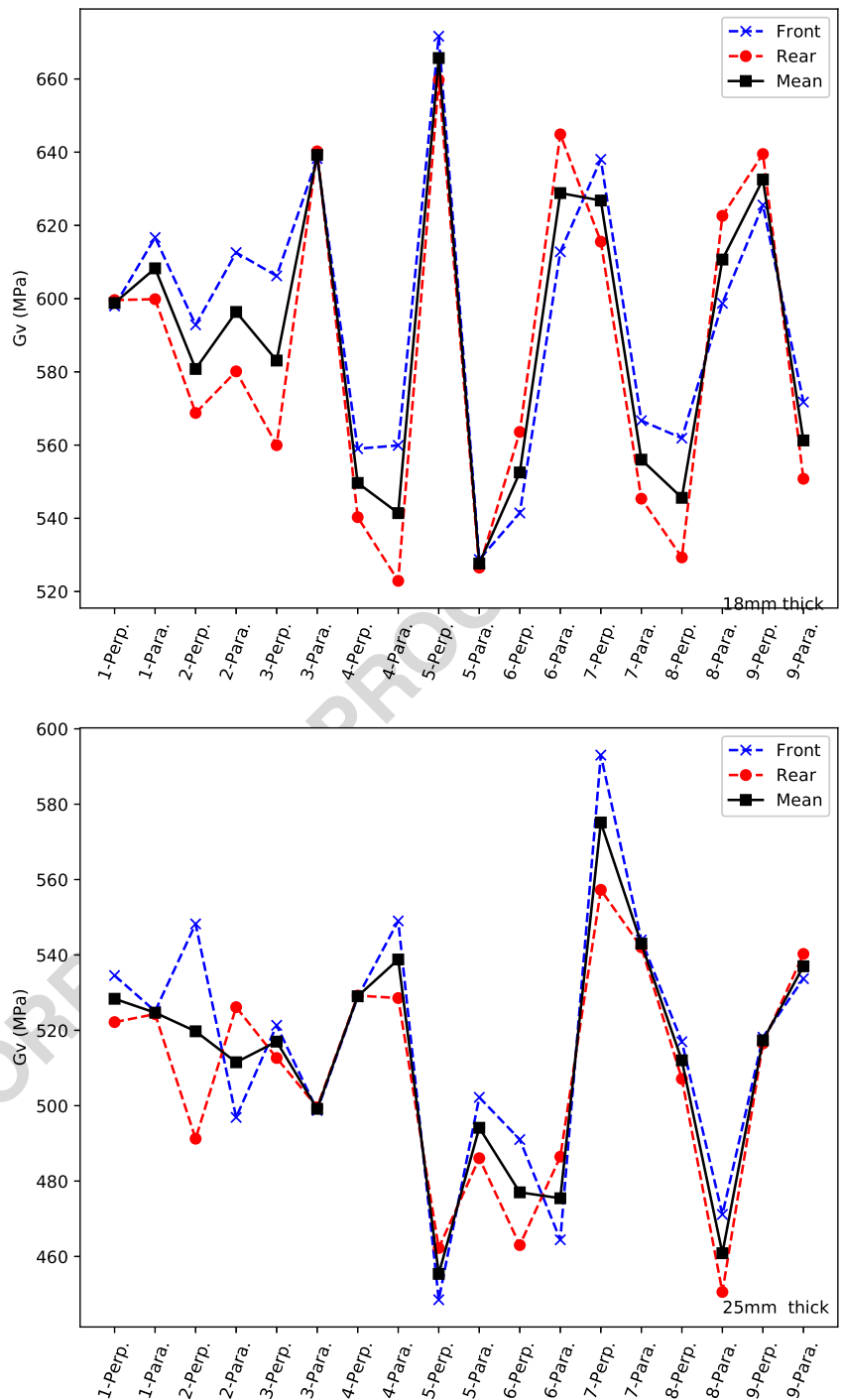
249 outcomes, it can be seen that the sample type Perpendicular
 250 has a higher shear modulus than the Parallel type. The
 251 difference observed between the sample types is higher for
 252 panels with a lower number of plies. These results highlight
 253 the homogenization process that occurs by increasing the
 254 number of plies. The shear modulus of rigidity is lower as
 255 the number of plies increases. The modeled shear modulus
 256 is increasing as the angle of the sample increases until

it reaches a maximum value (from 20° to 26° depending
 on the number of plies), then it decreases as the angle
 continues to increase. The relative variation of the shear
 modulus of rigidity for several tilting angles compared to
 the simulation with the non tilted configuration ($\alpha = 0^\circ$) is
 presented in Fig. 6. The variation is inferior to 20% in every
 cases. As the number of plies increases the relative variation
 also increases. The relative variation for an angle of 18°

257
 258
 259
 260
 261
 262
 263
 264



Fig. 10 Comparison of the shear modulus calculated on both side of the sample. The upper part is related to 18 mm thick samples and the lower part shows the results for 25 mm thick samples



265 is comprised between 11% and 17% for every modeled
 266 cases. This value has to be compared to a relative variation
 267 comprised between 10% and 15% for an angle equal to 14°
 268 as it was in the previous standard EN 789 (Fig. 1(b)).

Displacement Field and Shear Solicitation

The typical results obtained for a single test are presented in Fig. 7 (18 mm thick and Parallel type panel). The load-

269
 270
 271



Table 2 Minimum, mean, maximum, 5% percentiles values, standard deviations and coefficient of variation for different characterized properties

	Min	5% quant.	Mean	Max	SD	CV (%)
Density (kg.m ⁻³)						
18 mm thick.	661.9	682.4	717.7	752.2	18.3	2.5
Para.	699.7	695.5	720.7	741.2	11.9	1.6
Perp.	661.9	664.8	714.8	752.2	23.4	3.3
25 mm thick.	699.9	699.8	729.8	755.3	15.5	2.1
Para.	702.9	695.9	731.2	755.3	16.6	2.3
Perp.	699.9	695.9	728.5	746.9	15.3	2.1
All samples	661.9	690.9	723.8	755.3	17.8	2.5
G_v (MPa)						
18 mm thick.	520.8	506.2	587.6	665.7	42.1	7.2
Para.	527.6	500.4	585.5	639.2	40.0	6.8
Perp.	520.8	490.7	589.6	665.7	46.5	7.9
25 mm thick.	455.4	452.7	512.0	575.1	30.7	6.0
Para.	455.4	428.5	498.2	543.0	32.8	6.6
Perp.	494.1	478.2	525.7	575.1	22.4	4.3
All samples	455.4	452.5	549.8	665.7	52.8	9.6
f_v (MPa)						
18 mm thick.	10.5	10.5	12.0	13.1	0.7	6.1
Para.	10.5	10.1	11.8	12.9	0.8	6.7
Perp.	11.0	10.7	12.1	13.1	0.7	5.6
25 mm thick.	10.0	10.1	11.6	12.8	0.8	7.0
Para.	10.0	9.6	11.5	12.4	0.9	7.7
Perp.	10.8	10.2	11.8	12.8	0.7	6.2
All samples	10.0	10.4	11.8	13.1	0.8	6.6

272 displacement curves are presented in the upper part. The
 273 displacement represents the relative displacement of the two
 274 points as it was described before in the Section “**Mechanical**
 275 **Properties Calculation**” for each side of the panel (front and
 276 rear) analogously to the method described in EN 789. The
 277 two selected points are also visible on the displacements
 278 fields. The different steps for which displacements field
 279 are plotted correspond respectively to results under a load
 280 equal to $0.1 F_{max}$, $0.4 F_{max}$, $0.8 F_{max}$ and after failure under a
 281 residual load equal to $0.63 F_{max}$. For each step displacement
 282 fields in x-direction for both sides (Ux Front and Ux
 283 Rear) and in y-direction (Uy Front and Uy Rear) are
 284 presented. The measured displacement on both sides were
 285 really close to each other. This result can be seen on the
 286 load-displacement curve as well as on the displacement
 287 fields.

288 One of the advantages of DIC is that it allows to check
 289 the validity of the solicitation. The comparison of the
 290 displacements fields obtained on the front side by DIC and
 291 by FEM is presented in Fig. 8. The comparison is made at
 292 the same load and corresponds to the third step described
 293 previously (i.e at $0.8 F_{max}$). The comparison is done on the

294 displacements fields where the rigid body motion had been
 295 removed. It can be seen that the displacements fields in both
 296 directions were similar quantitatively.

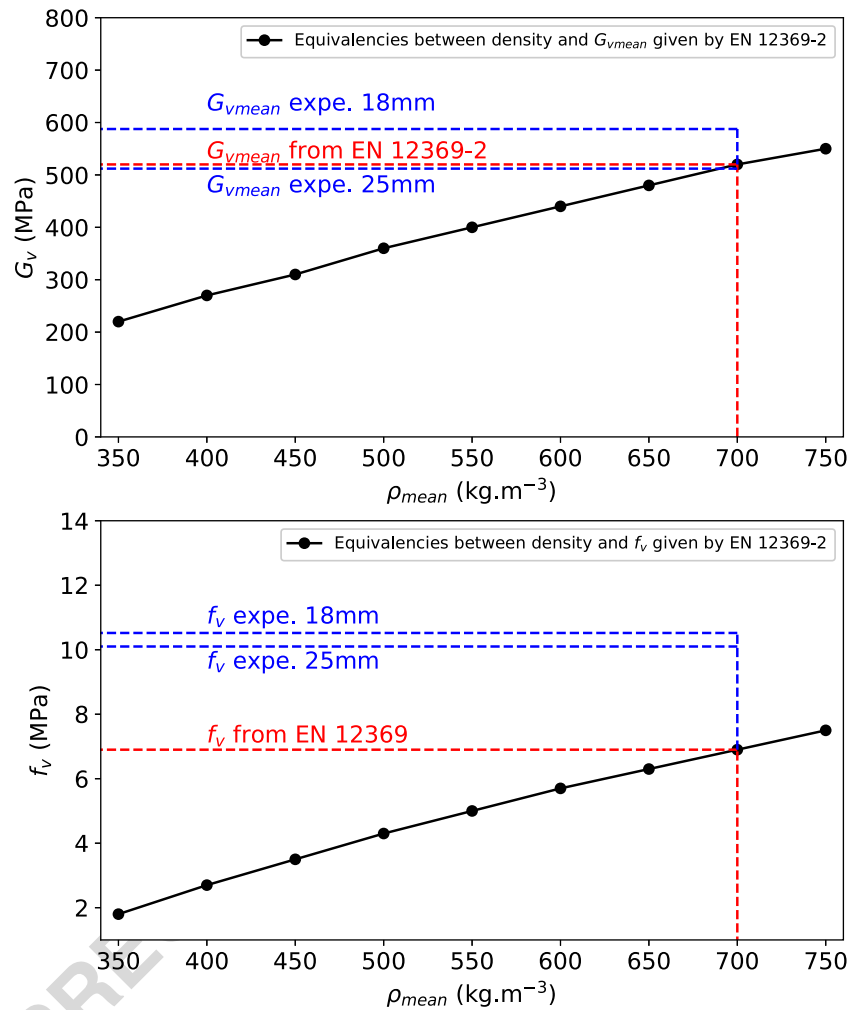
297 The lower part of Fig. 7 shows that this method is an
 298 effective way to identify the failure position. The failure
 299 position computed on the two sides of every samples is
 300 presented in Fig. 9. The distance from the centre and
 301 the actual failure path is comprised between -39.1 and
 302 32.1 mm. Therefore, every sample has been accepted for
 303 the computation of the shear strength since no failure
 304 occurred in another way than in shear between the two
 305 rails. The average absolute distance between the failure
 306 and the geometric centre is equal to 12.4 mm which can
 307 be considered low enough to use the shear length l in the
 308 calculation of the shear strength.

Mechanical Properties Analysis 309

310 Figure 10 presents the results of the shear modulus for
 311 the 36 panels, the upper part for the 18 mm thick panels
 312 and the lower part for the 25 mm thick panels. The blue
 313 dashed line represents the shear modulus calculated on the



Fig. 11 Comparison between experimental values and equivalencies given in EN 12369-2



314 basis of the DIC measurement on the front side, the red
 315 dashed line the one measured on the rear side, and the black
 316 plain line their mean value. Those results show that the
 317 difference between the shear modulus calculated on both
 318 sides is low. Indeed, the mean relative variation is equal to
 319 only 3.6% with a maximal relative variation equal to 13.7%.
 320 These percentages represent a mean absolute variation of
 321 20.2 MPa and a maximal variation of 76.5 MPa on the shear
 322 modulus.

323 Descriptive statistics for the density, the shear modulus,
 324 and the shear strength are given in Table 2. The mean value
 325 for 18 mm thick and 25 mm thick panel were respectively
 326 equal to 717.7 and 729.8 kg·m⁻³. The corresponding
 327 coefficients of variation were equal to 2.5 and 2.1% which
 328 is consistent with the literature in the case of beech [22–
 329 25]. The mean shear modulus G_v is respectively equal to
 330 587.6 and 512.0 MPa for 18 and 25 mm thick samples. This
 331 result is consistent with the results based on the numerical
 332 model. In addition, the samples from the type Perp. have
 333 a higher shear modulus in every case which is also in
 334 accordance with the numerical model. Finally, the average

335 shear strength f_v and its corresponding variability were
 336 really close for every thicknesses and sample types; the
 337 global averaged shear strength is approximately equal to
 338 12 MPa.

**Interest of the Test Realization Over Density Based
 Equivalencies**

341 The survey conducted on the plywood panel manufacturers’
 342 performances reports in Europe revealed that the majority
 343 of producers use density-based equivalencies given by the
 344 standards [8] to provide shear properties. The average
 345 densities for 18 mm and 25 mm thick panels were
 346 respectively 717 and 729 kg·m⁻³, according to the same
 347 standard the value of 700 kg·m⁻³ must be used (N.B:
 348 its lower limit must be used). Using this threshold, the
 349 shear properties could be taken equal to 520 and 6.9 MPa
 350 for the shear modulus and the shear strength respectively.
 351 Figure 11 presents the comparison between values obtained
 352 experimentally in this study and the values taken from the
 353 equivalencies applying the standards. These results show

354 that the realization of the shear tests is favorable or at least
 355 equivalent in the case of the shear modulus and always
 356 favorable for the calculation of the shear strength.

357 **Conclusion**

358 This study proposed a modified of the two rails shear test
 359 in a more functional configuration, meaning without the
 360 use of a bulky apparatus. The validity of the tests has
 361 been shown by the use of full field measurement using
 362 DIC. Nevertheless, the test could still be performed using a
 363 simpler measurement device such as a LVDT in the tilted
 364 proposed configuration. The interest of the realization of
 365 these tests has been highlighted in comparison with the use
 366 of equivalences based on the measurement of the average
 367 density. In any case, the measurements taken from the tests
 368 can lead to the declaration of shear properties equivalent
 369 or even greater than those expected by the standard
 370 and thus enhance significantly the valorization of beech
 371 plywood.

372 **Acknowledgements** The present study was financed by the company
 373 Fernand BRUGERE. This study was performed thanks to the
 374 partnership build by BOPLI: a shared public-private laboratory
 375 build between Bourgogne Franche-Compté region, LaBoMaP and the
 376 company Fernand BRUGERE. The authors would also like to thank
 377 the Xylomat Technical Platform from the Xylomat Scientific Network
 378 funded by ANR-10-EQPX-16 XYLOFOREST.

379 **Compliance with Ethical Standards**

380 **Conflict of interests** The authors declare that they have no conflict of
 381 interest.

382 **References**

383 1. Dobbin McNatt J (1969) Rail shear test for evaluating edgewise
 384 shear properties of wood base panel products. tech. rep., U.S.D.A
 385 Forest Service, Forest Products Laboratory. Madison
 386 2. Munthe B, Ethington RL (1968) Method for evaluating shear
 387 properties of wood. US Department of Agriculture, Forest Service,
 388 Forest Products Laboratory
 389 3. Rune Z (1994) Evaluation Of test methods for wood based panels.
 390 Determination of shear modulus and shear strength. Tech. Rep.
 391 Nordtest Project No. 1060–92, Swedish National Testing and
 392 Research Institute
 393 4. Ehlbeck J, Colling F (1984) Determination of panel shear
 394 strength and shear modulus of beech plywood in structural sizes.
 395 (SWITZERLAND)
 396 5. Wilson CR, Parasin AV (1979) A comparison of plywood modulus
 397 of rigidity determined by the ASTM and RILEM/CIB-3tt test
 398 methods. (Austria)
 399 6. Booth LG, Kuipers J, Noren B, Wilson CR (1977) Methods of
 400 test for the determination of mechanical properties of plywood,
 401 (Sweden)
 402 7. CEN (2005) EN 789 timber structures - test methods -
 403 determination of mechanical properties of wood based panels

8. CEN (2011) EN 12369-2 wood-based panels - characteristic 404
 values for structural design - Part 2: Plywood 405
 9. Yoshihara H, Yoshinobu M (2015) Young’s modulus and shear 406
 modulus of solid wood measured by the flexural vibration 407
 test of specimens with large height/length ratios. *Holzforschung* 408
 69(4):493–499 409
 10. Cavalli A, Marcon B, Cibecchini D, Mazzanti P, Fioravanti M, 410
 Procino L, Togni M (2017) Dynamic excitation and FE analysis 411
 to assess the shear modulus of structural timber. *Mater Struct* 412
 50(2):130 413
 11. Vacher P, Dumoulin S, Morestin F, Mguil-Touchal S (1999) 414
 Bidimensional strain measurement using digital images. *Proc Inst* 415
Mech Eng C J Mech Eng Sci 213(8):811–817 416
 12. Wattrisse B, Chrysochoos A, Muracciole J-M, Némoz-Gaillard M 417
 (2001) Analysis of strain localization during tensile tests by digital 418
 image correlation. *Exp Mech* 41(1):29–39 419
 13. Sutton M, Wolters W, Peters W, Ranson W, McNeill S 420
 (1983) Determination of displacements using an improved 421
 digital correlation method. *Image Vis Comput* 1(3):133– 422
 139 423
 14. Bruck H, McNeill S, Sutton MA, Peters W (1989) Digital image 424
 correlation using newton-Raphson method of partial differential 425
 correction. *Exp Mech* 29(3):261–267 426
 15. Bornert M, Brémand F, Doumalin P, Dupré J-C, Fazzini M, 427
 Grédiac M, Hild F, Mistou S, Molimard J, Orteu J-J, Robert L, 428
 Surré Y, Vacher P, Wattrisse B (2009) Assessment of digital 429
 image correlation measurement errors: methodology and results. 430
Exp Mech 49(3):353–370 431
 16. Jeong GY, Zink-Sharp A, Hindman DP (2009) Tensile properties 432
 of earlywood and latewood from loblolly pine (*Pinus taeda*) 433
 using digital image correlation. *Wood Fiber Sci* 41(1):51– 434
 63 435
 17. Zink AG, Davidson RW, Hanna RB (2007) Strain measurement in 436
 wood using a digital image correlation technique. *Wood Fiber Sci* 437
 27(4):346–359 438
 18. Haldar S, Gheewala N, Grande-Allen K, Sutton M, Bruck 439
 H (2011) Multi-scale mechanical characterization of palmetto 440
 wood using digital image correlation to develop a template for 441
 biologically-inspired polymer composites. *Exp Mech* 51(4):575– 442
 589 443
 19. CEA (2019) Cast3m 444
 20. Guitard D (1987) Mécanique du matériau bois et composites. 445
 NABLA, cepadues ed. 446
 21. Bergman R, Cai Z, Carll CG, Clausen CA, Dietsberger MA, 447
 Falk RH, Frihart CR, Glass SV, Hunt CG, Ibach RE (2010) Wood 448
 handbook: Wood as an engineering material. Forest Products 449
 Laboratory 450
 22. Gérard J, Guibal D, Paradis S, Vernay M, Beauchêne J, 451
 Brancheriau L, Châlon I, Daigremont C, Détienne P, Fouquet D, 452
 Langbour P, Lotte S, Thévenon M-F, Méjean C, Thibaut A (2011) 453
Tropix 7 454
 23. Pöhler E, Klingner R, Künniger T (2006) Beech (*Fagus sylvatica* 455
 L.) – Technological properties, adhesion behaviour and colour 456
 stability with and without coatings of the red heartwood. *Annals* 457
Forest Sci 63(2):129–137 458
 24. Viguier J, Bourgeay C, Rohumaa A, Pot G, Denaud L (2018) 459
 An innovative method based on grain angle measurement to sort 460
 veneer and predict mechanical properties of beech laminated 461
 veneer lumber. *Constr Build Mater* 181:146–155 462
 25. Viguier J, Marcon B, Girardon S, Denaud L (2017) Effect 463
 of forestry management and veneer defects identified by x-ray 464
 analysis on mechanical properties of laminated veneer lumber 465
 beams made of beech. *BioResources* 466

Publisher’s Note Springer Nature remains neutral with regard to 467
 jurisdictional claims in published maps and institutional affiliations. 468

